

Signature of a Type-A Glass Transition and Intrinsic Confinement Effects in a Binary Glass-Forming System

Thomas Blochowicz,^{1,*} Sebastian Schramm,¹ Sorin Lusceac,¹ Michael Vogel,¹ Bernd Stühn,¹
Philipp Gutfreund,² and Bernhard Frick²

¹*Institut für Festkörperphysik, Technische Universität Darmstadt, 64289 Darmstadt, Germany*

²*Institut Laue Langevin, 38043 Grenoble, France*

(Received 14 December 2011; published 20 July 2012)

We study dynamically highly asymmetric binary mixtures comprised of small methyl tetrahydrofuran (MTHF) molecules and polystyrene. Combined use of dielectric spectroscopy, ²H nuclear magnetic resonance, incoherent quasielastic neutron scattering, and depolarized dynamic light scattering allows us to selectively probe the dynamics of the components in a broad dynamic range. It turns out that the mixtures exhibit two glass transitions in a wide concentration range although being fully miscible on a macroscopic scale. In between both glass transition temperatures, the dynamics of the small molecules show strong confinement effects, e.g., a crossover from Vogel-Fulcher to Arrhenius behavior of the time constants. Moreover, the dynamical behavior of small molecules close to the slow matrix is consistent with mode coupling theory predictions for a type-A glass transition, which was expected from recent theoretical and simulation studies in comparable systems.

DOI: [10.1103/PhysRevLett.109.035702](https://doi.org/10.1103/PhysRevLett.109.035702)

PACS numbers: 64.70.pm, 77.22.Gm, 29.30.Hs

Binary glass-forming systems have many applications, as material properties can be tailored by adapting the composition. However, fundamental properties are still poorly understood, especially for mixtures of unlike partners with a high dynamic asymmetry, i.e., a large difference in the glass transition temperatures T_g of the components. Traditionally it was assumed that two components mix well only if the binary system shows a single T_g [1]. Recent studies, however, identified two calorimetric glass transition temperatures, and thus a separation of time scales, in fully miscible systems [2,3]. In that case intrinsic confinement effects have to be expected, when a more mobile component relaxes in a matrix of slow or even frozen larger molecules. It is the aim of the present contribution to investigate such intrinsic confinement effects in the dynamics of the mobile component in binary mixtures of weakly interacting van der Waals liquids.

Experimentally, the dynamics of the mobile molecules in a binary mixture shows signatures of the existence of the slower or static matrix, akin to confinement effects observed for glass formers in nanoporous materials. For confined liquids, deviations from a Vogel-Fulcher temperature dependence were reported for the structural relaxation times [4] and very prominent dynamical heterogeneities were found [5]. However, it is still unclear, to what extent the observations are due to particular interactions at the liquid-solid interface or to spatial restrictions in confinement [6]. In particular, for water in nanoporous materials or protein matrices, the existence and the interpretation of crossovers in temperature-dependent correlation times was vigorously debated in recent years [7,8]. In mixtures of van der Waals liquids, as in the present study, one may clarify to what extent such a crossover has to be regarded as a general confinement induced phenomenon.

The separation of time scales, which underlies the confinement effects in binary mixtures, has important implications for a wide spectrum of materials, extending from polymeric ion conductors to hydrated proteins. And yet, its origin is still a matter of ongoing debate. For polymer blends, e.g., it was explained in terms of local concentration variations [9]. An alternative picture is given by the mode coupling theory (MCT), a major microscopic theory that attempts to describe the glass transition [10]. In bulk liquids the theory predicts the existence of a critical temperature $T_c > T_g$ at which the structural α -relaxation time diverges and the long time limit f of the density autocorrelation function, the so-called nonergodicity parameter, shows a discontinuous jump from 0 to $f_c > 0$. This scenario is called a *type-B* glass transition. For binary mixtures, on the other hand, MCT predicts an intrinsic difference in mobility for sufficiently disparate large and small particles [11]. And for the dynamics of the confined mobile particles a so-called *type-A* scenario emerges: In that case the nonergodicity level increases continuously from zero upon cooling below T_c , approximately as $f \propto T_c - T$. The existence of such a type-A transition was predicted not only for translational motion of mobile particles inside a slow matrix [11,12], but also for rotational motion [13] and it was recently identified in simulation studies [14]. In the present work, we show its relevance for the dynamics of the mobile component in molecular binary glass formers.

We apply various spectroscopic techniques to investigate mixtures of 2-methyl tetrahydrofuran (MTHF) with Oligo- and Polystyrenes (PS) of different molecular weights M_w . Protonated polymers were purchased from Polymer Standards Service (Mainz, Germany) and perdeuterated PS was obtained from Polymer Source (Montreal,

Canada). Protonated MTHF was obtained from Acros Organics, while ring-deuterated MTHF- d_7 and methyl-group-deuterated MTHF- d_3 were synthesized by H. Zimmermann (MPI, Heidelberg) [15].

Differential scanning calorimetry measurements were performed on a DSC Q-1000 from TA Instruments. Heating runs at a rate of 30 K/min were recorded and the inflection points of the heat flow were taken as glass transition temperatures. Although MTHF and PS are miscible over the full concentration and temperature range [3], two glass transitions can be clearly identified for mixtures with MTHF weight fractions of $c < 70\%$, as demonstrated for a typical example in the inset of Fig. 1.

The upper glass transition temperature in the styrene MTHF mixtures shows a pronounced dependence on solvent fraction and PS molecular weight M_w , whereas the lower one only slightly depends on these parameters. The dynamic asymmetry, i.e., the difference in the component glass transitions is enhanced by increasing M_w of PS in several steps from the distilled trimer (TS) to M_w of 1900 (PS2k), 60 000 (PS60k), and 78 000 (PS80k) g/mol. Although qualitatively the overall behavior remains the same for each M_w , the gap between the two T_g s and thus the region, where intrinsic confinement effects are expected, increases with growing chain length. Traditionally, different phenomenological expressions were used to interpolate mixture T_g s. Figure 1 shows as solid line: $T_g^{\text{mix}}(c) = cT_g^{\text{MTHF}} + (1-c)T_g^{\text{TS}} - Kc(1-c)$ [16] applied to the upper T_g of the TS mixtures. In these data the apparent crossover, which is modelled by the phenomenological description, is due to the merging of the two linear T_g traces in the intermediate concentration range. Thus, it is likely that a region with a second T_g and corresponding intrinsic confinement are present in many more

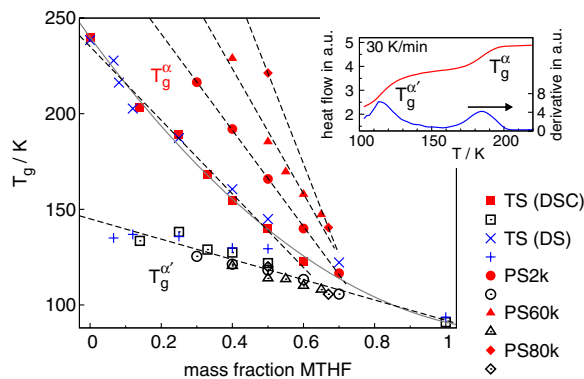


FIG. 1 (color online). Glass transition temperatures T_g^α and $T_g^{\alpha'}$ for various MTHF-PS mixtures. The T_g values of pure MTHF [21] and TS are included. Open and full symbols: T_g values derived from DSC measurements, crosses: T_g values derived from DS data. The lines are fits of the concentration dependences of T_g^α and $T_g^{\alpha'}$ (dashed, linear interpolations; solid, see text with $K = 104$ K). Inset: DSC curve together with its derivative for a mixture of 50% MTHF and PS60k.

mixed systems and just may have been overlooked when analyzing the data in a traditional way.

From the M_w dependence and from an extrapolation of the concentration dependence to the limit of neat components, one is tempted to conclude that each of the two glass transitions is related to the respective molecular dynamics of one of the components. To check this and to gain detailed insights into the relaxation processes of the components, we apply various experimental techniques that selectively probe the dynamical behavior of one of the molecular species in the following.

First, we use dielectric spectroscopy (DS) to monitor the dynamics of MTHF, exploiting the fact that the dipole moment of PS is negligibly small with respect to that of MTHF. Dielectric measurements were performed using a Novocontrol Alpha-N Analyzer. Figure 2 (left) shows the dielectric loss for a mixture of 50% MTHF and PS60k. Between 110 and 250 K, three dynamical processes are resolved, which are analyzed with a set of previously described phenomenological relaxation time distributions [3]. In Fig. 3, the resulting time constants are compared with time constants from the calorimetric measurements, as calculated following Hodge [17]. We see that the two calorimetric glass transitions are associated with the two slowest dielectric processes, which are, thus, denoted as α and α' relaxation in the following, while the fastest dielectric process can be identified with the Johari-Goldstein β -relaxation of MTHF; see [3].

Information about the molecular origin of the α -relaxation is available from depolarized dynamic light scattering (DDLS), which is sensitive to the reorientation of the anisotropic part of the polarizability tensor and thus probes the segmental reorientation of PS in the studied mixtures. Therefore, we performed photon correlation spectroscopy in VH-geometry using a standard setup in combination with a cold-finger cryostat. The correlation functions resulting for the 50% MTHF-PS60k mixture show a single, angle-independent, nonexponential relaxation, with $\beta_{\text{KWW}} \approx 0.4$ indicating only slight broadening compared to the neat polymer. The average relaxation times τ_α from DS and DDLS agree very well; see Fig. 3. Moreover the calorimetric time constant extracted at the upper T_g exactly matches the $\tau_\alpha(T)$ trace indicating that the glass transition of the large PS molecules is at the origin of the α -relaxation of the mixture, resulting in a formation of a glassy styrene matrix around the upper T_g .

However, this is not the end of the story. Further insights can be obtained when we analyze the relaxation strengths of the various dielectric processes observed for the 50% MTHF-PS60k mixture. First, we consider the total relaxation strength $\Delta\varepsilon_{\text{tot}}(T) = \varepsilon_s(T) - \varepsilon_\infty$, where the instantaneous contribution ε_∞ and the static permittivity ε_s are extracted from the real part $\varepsilon'(\nu)$ of the dielectric data. In Fig. 4, we see that the trivial temperature dependence is removed when plotting the relaxation strength

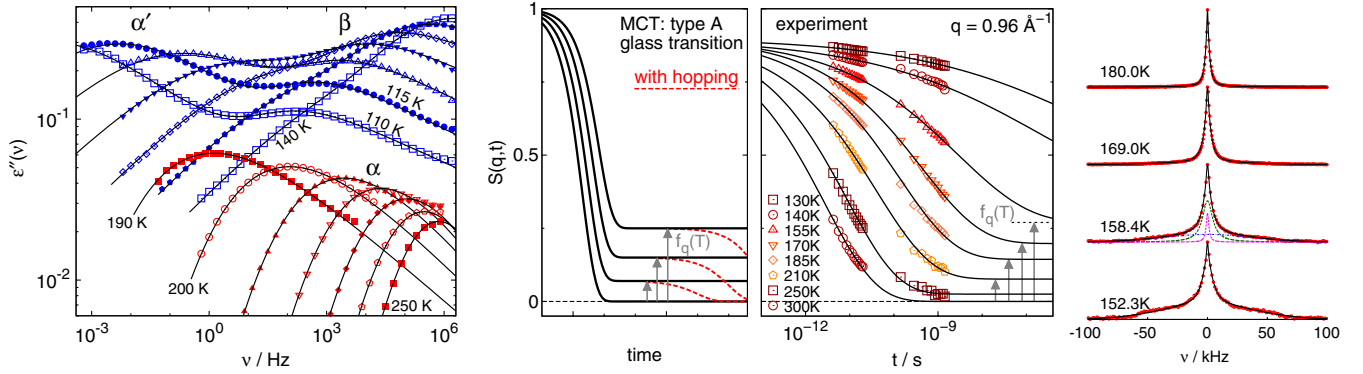


FIG. 2 (color online). *Left*:—Frequency-dependent dielectric loss of 50% MTHF in PS60k. The α relaxation is seen in the high temperature data (190–250 K, lower red points) while the low-temperature data (110–140 K, upper blue points) show the α' and β processes. The lines are fits with appropriate model functions [22]. *Middle*:—Sketch of the MCT type-A glass transition with and without hopping, and incoherent scattering functions of 50% MTHF-d₃ in PS60k-d₈. Fits with a KWW function and a plateau value estimated from the dielectric data. *Right*:—Temperature-dependent ²H NMR solid-echo spectra of 45% MTHF-d₇ in PS60k.

as $(T - T_\delta)\Delta\epsilon_{\text{tot}}(T)$, where a finite value $T_\delta \approx 60$ K indicates a Curie-Weiss type temperature dependence. More importantly, it is evident in Fig. 4 that, at sufficiently low temperatures, the relaxation strength of the α process, $\Delta\epsilon_\alpha$, is much larger in the mixture than the contribution $\Delta\epsilon_{\text{PS}}$ expected from neat PS, implying that, in addition to PS, MTHF contributes to the α process. It was shown previously in MTHF-tristyrene mixtures that the overall relaxation strength varies as a linear function of MTHF concentration in the range of 0–0.7 mass fraction MTHF (see Fig. 5 in [3]). Therefore, the above argument holds even though, in general, dielectric permittivities are not necessarily additive in binary mixtures.

A comparison of $\Delta\epsilon_\alpha$ with data for neat PS reveals that the temperature dependence of $\Delta\epsilon_\alpha$ in the mixture strongly differs from what is known in neat glass-forming liquids. We note that $\Delta\epsilon_\alpha(T)$ consistently extrapolates towards lower temperatures, e.g., at 125 K the combined relaxation

strength of the α' and β processes, $\Delta\epsilon_{\alpha'+\beta}$, together with the extrapolated $\Delta\epsilon_\alpha$ again yields $\Delta\epsilon_{\text{tot}}$.

To follow the dynamics of MTHF to higher temperatures, we apply quasielastic neutron scattering (QENS) to a mixture of 50% MTHF-d₃ with perdeuterated PS60k, so that the incoherent scattering of the protonated ring of MTHF-d₃ dominates the total scattering cross section and, hence, the ring motion of MTHF is selectively probed. Combination and Fourier-transformation of dynamic structure factors $S(q, \omega)$, which were measured at the IN5 and IN16 spectrometers at the Institute Laue-Langevin (Grenoble, France), yield a dynamic range from 1 ps to 2 ns. The appropriate wave vector for a comparison of DS and QENS data can be determined by comparison of the respective time constants for neat MTHF. In agreement with previous findings in many different systems [18,19], a common Vogel-Fulcher behavior is obtained for $q \approx 1 \text{ \AA}^{-1}$; see Fig. 3. Figure 2 shows intermediate scattering functions $S(q, t)$ of the mixture at this scattering vector. Consistent

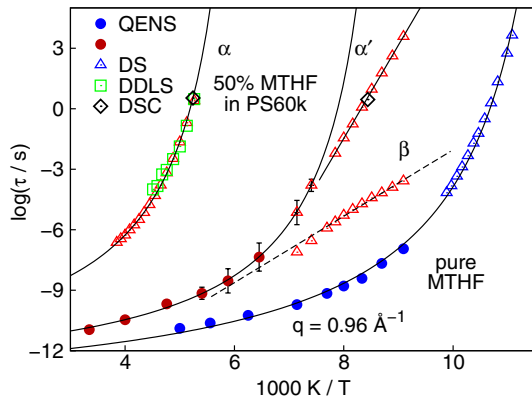


FIG. 3 (color online). Relaxation times of the dynamic processes observed for 50% MTHF in PS60k and for pure MTHF employing DS, QENS, DDLS, and DSC. DS, and QENS data match for the used scattering vector $q = 0.96 \text{ \AA}^{-1}$. Solid and dashed lines are fits with Vogel-Fulcher and Arrhenius laws, respectively.

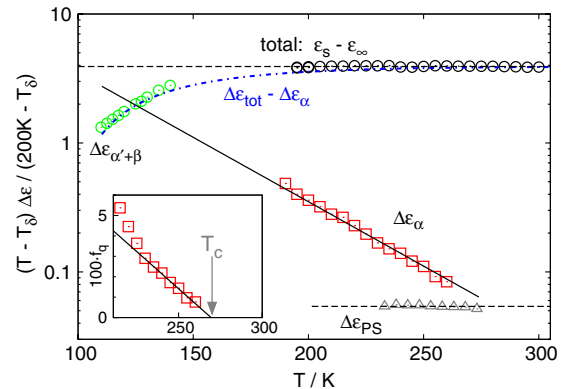


FIG. 4 (color online). Dielectric relaxation strengths $\Delta\epsilon$ of the observed dynamical processes corrected for the temperature dependence of the overall relaxation strength $\Delta\epsilon_{\text{tot}}$. The inset shows $f_q \approx (\Delta\epsilon_\alpha - \Delta\epsilon_{\text{PS}}) / \Delta\epsilon_{\text{tot}}$. The line is a fit of the MCT prediction for a type-A glass transition, yielding $T_c \approx 269$ K.

with the calorimetric and dielectric data, there is significant decorrelation at short times even at $T < T_g^\alpha$. As the above discussion of $\Delta\varepsilon_\alpha$ showed that MTHF contributes to the slow α relaxation, a part of the orientational correlation is lost outside the dynamic range of QENS. Thus, $S(q, t)$ should exhibit an elastic contribution. To include the latter in the analysis of $S(q, t)$ we added $f_q \approx (\Delta\varepsilon_\alpha - \Delta\varepsilon_{\text{PS}})/\Delta\varepsilon_{\text{tot}}$ as a fixed elastic contribution estimated from the dielectric data to the KWW fits of QENS. The resulting curves are shown in Fig. 2 (middle) and the time constants are included in Fig. 3. Note that the error bars shown with the full circles include the uncertainty introduced by the fact that the true plateau values are not known exactly.

Of course, the plateau values f_q may in principle differ for dielectric and neutron data. Nevertheless, our approach to calculate the elastic contribution from the dielectric relaxation strengths yields a very good description of $S(q, t)$ and, hence, a consistent description of both dielectric and scattering data is achieved. Interestingly, the plateau value, i.e., $\Delta\varepsilon_\alpha - \Delta\varepsilon_{\text{PS}}$ continuously tends to zero upon increasing temperature while τ_α is in the microsecond regime. We interpret this continuous crossover of f_q as the signature of a type-A glass transition: While being zero at high temperatures, f_q increases below T_c . In the inset of Fig. 4, we see that, in the vicinity of T_c , the expected asymptotic relation $f_q \propto T_c - T$ holds to good approximation and leads to $T_c \approx 269$ K.

As is common for molecular systems, at $T < T_c$ a finite value of f_q does not indicate a crossover to a real non-ergodic state, but hopping processes are usually thought to restore ergodicity, as outlined in Fig. 2(middle). In the present system, a finite plateau most likely results from small molecules being motionally restricted in the vicinity of the slow matrix. Hence, the final correlation decay should coincide with the loss of the matrix correlations during the α relaxation. And indeed, the dynamics of the PS molecules observed in DDLS and the final loss of orientational correlation of the MTHF molecules found in DS occur on the same time scale, cf. Fig. 3.

In theoretical and simulation studies, a type-A glass transition scenario usually results for low concentrations of mobile particles, while a crossover to a type-B behavior is found at higher concentrations [13,14,20]. For the present mixtures, we propose that two distinct species of MTHF molecules exist at the same time: While small molecules in the vicinity of the matrix exhibit type-A behavior, i.e., residual correlation until the matrix structure relaxes, small molecules at a larger distance from the matrix show a type-B like scenario (α' process), which is, however, influenced by confinement effects, particularly at temperatures below the upper glass transition, which manifest themselves in a crossover from a Vogel-Fulcher to an Arrhenius temperature dependence for $\tau_{\alpha'}$.

To further clarify the microscopic nature of the α - and α' -relaxations, we applied ^2H NMR to a mixture of 45%

MTHF-d₇ and PS60k so that the motion of the MTHF rings is probed. In ^2H NMR, a broad and a narrow spectrum is observed when molecular dynamics is slow and fast on the timescale of 10^{-6} s, respectively. In Fig. 2(right), we show ^2H NMR spectra at temperatures, where $\tau_\alpha \gg 10^{-6}$ s and, hence, the α process does not result in motional narrowing. Nevertheless, a narrow spectrum is observed at 180 K, indicating that the α' process determines the line shape, consistent with $\tau_{\alpha'} \ll 10^{-6}$ s, see Fig. 3. The absence of a broad spectral component reveals that essentially all MTHF molecules participate in the α' process. When the temperature is decreased, a broad line gains intensity, indicating that an increasing fraction of MTHF molecules become immobile due to the broad α' -relaxation crossing the NMR time window. The shape of the broad line deviates from that of the typical solid-state spectrum due to effects of ring puckering motions [3]. Closer analysis of the narrow line shows that the latter has two contributions. Hence, two species of MTHF molecules exist, for which the α' -process differs with respect to the time scale and/or the geometry of the underlying motion. Thus, the increasing value of f_q in DS and QENS is not due to immobilized small molecules but rather related to a fraction of MTHF most likely residing close to the PS matrix that shows increasingly hindered and anisotropic motion upon cooling.

In conclusion, we have shown that confinement effects play an important role in binary mixtures with a large dynamic asymmetry, here in MTHF-PS mixtures. Below the glass transition of the matrix, the MTHF molecules exhibit fast reorientation characterized by a weak anisotropy and a crossover from Vogel-Fulcher to Arrhenius temperature dependence of the relaxation times. The dielectric relaxation of a fraction of MTHF molecules, most probably of molecules close to the matrix, clearly shows signatures of a type-A glass transition, including a continuous increase of a nonergodicity level below the critical temperature T_c . So far, such behavior was anticipated in MCT and MD simulation studies in simple mixtures and confinements [11–14,20]. Combining results from DS and NMR with neutron and light scattering data, we argue that, in the present system, the type-A glass transition is related to the effect that reorientation of MTHF molecules close to the PS matrix is not isotropic until the matrix structure relaxes.

We are indebted to R. Böhmer (Dortmund) and H. Zimmermann (Heidelberg) for providing the partially deuterated MTHF samples. Furthermore, financial support of the Deutsche Forschungsgemeinschaft in the framework of FOR 1583 and of Grant No. BL 923/1 is gratefully acknowledged.

*thomas.blochowicz@physik.tu-darmstadt.de

[1] L. A. Utracki, *Polymer Alloys and Blends: Thermodynamics and Rheology* (Hanser Verlag, Munich, 1989).

- [2] T. P. Lodge, E. R. Wood, and J. C. Haley, *J. Polym. Sci., Part B: Polym. Phys.* **44**, 756 (2006).
- [3] T. Blochowicz, S. A. Lusceac, S. Schramm, P. Gutfreund, and B. Stühn, *J. Phys. Chem. B* **115**, 1623 (2011).
- [4] A. Schönhals, H. Goering, C. Schick, B. Frick, M. Mayorova, and R. Zorn, *Eur. Phys. J. Special Topics* **141**, 255 (2007).
- [5] B. Frick, C. Alba-Simionesco, G. Dosseh, C. LeQuellec, A. J. Moreno, J. Colmenero, A. Schönhals, R. Zorn, K. Chrissopoulou, S. H. Anastasiadis, and K. Dalnoki-Veress, *J. Non-Cryst. Solids* **351**, 2657 (2005).
- [6] G. B. McKenna, *Eur. Phys. J. Special Topics* **141**, 291 (2007).
- [7] S.-H. Chen, L. Liu, E. Fratini, P. Baglioni, A. Faraone, and E. Mamontov, *Proc. Natl. Acad. Sci. U.S.A.* **103**, 9012 (2006).
- [8] W. Doster, S. Busch, A. M. Gaspar, M.-S. Appavou, J. Wuttke, and H. Scheer, *Phys. Rev. Lett.* **104**, 098101 (2010).
- [9] J. Colmenero and A. Arbe, *Soft Matter* **3**, 1474 (2007).
- [10] W. Götze and L. Sjögren, *Rep. Prog. Phys.* **55**, 241 (1992).
- [11] Y. Kaneko and J. Bosse, *J. Non-Cryst. Solids* **205–207**, 472 (1996).
- [12] V. Krakoviack, *Phys. Rev. Lett.* **94**, 065703 (2005).
- [13] S.-H. Chong, W. Götze, and A. P. Singh, *Phys. Rev. E* **63**, 011206 (2000).
- [14] K. Kim, K. Miyazaki, and S. Saito, *Eur. Phys. J. Special Topics* **189**, 135 (2010).
- [15] F. Qi, T. El Goresy, R. Böhmer, A. Döb, G. Diezemann, G. Hinze, H. Sillescu, T. Blochowicz, C. Gainaru, E. A. Rössler, and H. Zimmermann, *J. Chem. Phys.* **118**, 7431 (2003).
- [16] J. M. Gordon, G. B. Rouse, J. H. Gibbs, and W. M. Risen, *J. Chem. Phys.* **66**, 4971 (1977).
- [17] I. M. Hodge, *J. Non-Cryst. Solids* **169**, 211 (1994).
- [18] T. Blochowicz, E. Gouirand, A. Fricke, T. Spehr, B. Stühn, and B. Frick, *Chem. Phys. Lett.* **475**, 171 (2009).
- [19] J. Colmenero, A. Arbe, and A. Alegría, *J. Non-Cryst. Solids* **172–174**, 126 (1994).
- [20] T. Voigtmann and J. Horbach, *Phys. Rev. Lett.* **103**, 205901 (2009).
- [21] M. Mizukami, H. Fujimori, and M. Oguni, *Prog. Theor. Phys. Suppl.* **126**, 79 (1997).
- [22] T. Blochowicz, C. Tschirwitz, S. Benkhof, and E. A. Rössler, *J. Chem. Phys.* **118**, 7544 (2003).